# AC conductivity and dielectric analysis of $Pb_{1-x}La_x[(Mg1+x/3Nb_{2-x/3})_{0.65}Ti_{0.35(1-x)/4}]O_3$, (x = 0, 0.02, 0.05) relaxor ferroelecric ceramics

**Pragya Pandit1*, Pargin Bangotra[2]**

[1]*Atomic Minerals Department for Exploration and Research, Department of Atomic Energy, Delhi, 110066, India*
[2]*National Institute of Technology, Department of Physics, Jalandhar, Punjab, 144011, India*

*Corresponding author, E-mail: pragyapandit.amd@gov.in

**Received: 31 March 2016, Revised: 02 August 2016 and Accepted: 03 September 2016**

DOI: 10.5185/amp.2016/204
www.vbripress.com/amp

## Abstract

In this paper we investigate the effect of lanthanum doping on structural, dielectric and electrical properties of lead magnesium niobate - lead titanate, $0.65Pb(Mg_{1/3}Nb_{2/3}O_3)$- $0.35PbTiO_3$ (x=0, 0.02, 0.05) ferroelectric ceramics. Dielectric and AC impedance spectroscopic measurements were carried out on pure and lanthanum doped PMN/PT ceramics over a wide temperature ($30^o$- $450^o$ C) and frequency interval (10 Hz-1 MHz). Pure and lanthanum doped $Pb_{1-x}La_x[(Mg_{1+x/3}Nb_{2-x/3)0.65}Ti_{0.35(1-x/4)}]O_3$, (x=0, 0.02, 0.05) ceramics were prepared by solid state reaction route using columbite precursor method. X-ray diffraction revealed tetragonal (P4mm) phase for pure PMN/PT ceramics and transition to pseudo cubic phase (Pm3m) was observed with increased lanthanum doping. The dielectric response of the lanthanum modified PMN/PT ceramics was interpreted in terms of modified curie weiss law. Modulus spectroscopy revealed the deviation of dielectric behavior from ideal Debye behaviour. Activation energies calculated from dielectric relaxation and modulus spectroscopy suggested that charge transport processes are due to oxygen ion hopping.The AC conductivity of the PMN/PT ceramics initially increased for 2 mol% of lanthanum doping followed by a subsequent decrease with further 5 mol% of lanthanum doping. The value of the activation energies calculated from the temperature dependance of ac conductivity was in the range from 1.20-1.48 ev which is due to doubly ionized oxygen vacancies. The overall structural, electrical and dielectric behaviour of $Pb_{1-x}La_x[(Mg_{1+x/3}Nb_{2-x/3)0.65}Ti_{0.35(1-x/4)}]O_3$, (x=0, 0.02, 0.05) ceramics is correlated to the relaxor nature induced by lanthanum doping. Copyright © 2016 VBRI Press

**Keywords:** Ferroelectrics, solid solution route, dielectric properties, AC conductivity, impedance.

## Introduction

Relaxor based ferroelectric ceramic Lead Magnesium Niobate-Lead Titanate $Pb(Mg_{1/3}Nb_{2/3})O_3$-$PbTiO_3$ (PMN-PT) is extensively studied due to its excellent dielectric, pyroelectric and electromechanical properties **[1-3]**. Due to relaxor ferroelectric nature PMN-PT exhibits frequency dependent diffuse phase transition, deviation from curie weiss law in low field dielectric measurements, low hysterctic losses in high field polarization measurements and presence of polar nanodomains at temperature well above the curie temperature. As a result it finds applications in multilayer capacitors, ultrasonic transducers, actuators and as smart materials **[4, 5]**. Lead Magnesium niobate (PMN) is an archetypical relaxor ferroelectric material (Tc = $-15^oC$) with rhomohedral symmetry and readily forms a solid solution with normal ferroelectric, lead titanate (PT) (Tc = $490^oC$) of tetragonal symmetry with their morphotropic phase boundary (MPB) located at 33-35% PT **[6-8]**. MPB compositions exhibit best electrical and piezoelectric properties and are are technologically important due to the coexistence of phases. The normal ferroelectric behaviour of PMN-PT is retained till the morphotropic boundary (MPB) composition corresponding to 65PMN-35PT **[9]**. Addition of PMN greater than 65 mol% leads to the onset of relaxor ferroelectric behaviour.

The relaxor nature of PMN-PT is attributed to the structural, chemical and compositional inhomogenties. Several models such as random field model, spherical random bond random field model have been proposed to explain the relaxor ferroelectric nature of PMN **[10, 11]**. According to these models the relaxor nature in these materials arises due to the inherent charge imbalance problem created by B site disorder. Charge imbalance in these materials leads to the formation of chemical and polar clusters. The alternating (111) sites in PMN-PT are occupied by $Mg^{2+}$ or $Nb^{5+}$ with overall

stochiometric ratio of 1:2. Since each unit cell requires an ion of valence 4+ at the body center for charge balancing. As a result there are small regions with 1:1 chemical ordering called chemical clusters extending over 2-10 nm separated by Nb rich regions. These stochiometric chemical clusters $[Pb(Mg_{1/2}Nb_{1/2})]O_3$ carry an effective negative charge of 0.5e per unit cell whereas the Nb rich regions or polar clusters carry an effective positive charge. Since these chemical and polar clusters are compositionally different hence different dynamically variable nucleation sites are available for the emergence of new phases on cooling towards the curie temperature, Tc leading to highly diffuse phase transition characteristic of relaxor materials.

External electric field and doping with higher valent ions at the A site in PMN-PT is said to influence the chemical and polar clusters and hence the relaxor ferroelectric nature of PMN-PT. Lanthanum ($La^{3+}$) substitution of PMN-PT at both A ($Pb^{2+}$) and B site ($Ti^{4+}$) leads to the enhancement in the relaxor nature due to increase in the size of the chemical clusters and simultaneously a decrease in the size of the polar clusters. While lanthanum($La^{3+}$) substitution at A site of the perovskite unit cell replaces some of the $Pb^{2+}$ at the corners of the unit cell and the charge compensation resulting from this substitution results in, either a defect complex bound to the Pb vacancy whereas the lanthanum($La^{3+}$) substitution at the B site leads to enhanced charge imbalance problem due to the successive deviation from the 4+ value required than the average value of 3.5+ coming from $Mg^{2+}$ and $Nb^{5+,}$which again enhances the relaxor nature **[12]**.

Though various articles have been published on the effect of lanthanum doping on the structural, optical, electrooptical and electrical properties of PMN/PT and AC impedance spectroscopy properties of 65/35 PMN/PT ceramics **[13-15]**, no specific study has so far conducted to see the effect of lanthanum doping on the ac conduction studies of PMN/PT. S. M. Gupta et al. have conducted the impedance spectroscopic study of $Pb_{1-x}\ La_x\ [(Mg_{1+x/3}\ Nb_{2-x/3}\ )_{0.65}Ti_{0.35(1-x/4)}]O_3$ ceramic s, with x = 0 to 0.07 where higher resistive and lower capacitive grain and grain boundaries are known to induce relaxor nature **[16]**. Based on our knowledge this is the first study on the temperature dependent AC conductivity of pure and lanthanum doped PMN/PT ceramic in wide frequency interval to understand the effect of lanthanum on the conduction mechanism of PMN/PT.

Complex impedance spectroscopy is a very useful tool to evaluate the electrical behaviour of polycrystalline samples **[17, 18]**. In the present study complex impedance spectroscopy has been performed on materials to evaluate the effect of lanthanum doping on the ac and dc conductivity of the PMN/PT ceramic samples. Dielectric properties are correlated with relaxor nature of the ceramics. The role of lanthanum doping on relaxation and dielectric behavior of PLMNTx (x=0, 0.02 & 0.05) (abbreviated afterwards 65/35, 2/65/35 and 5/65/35 PMN/PT) ceramics has been described. Simultaneously the effect of Lanthanum doping on the conductivity in 65/5,2/65/3 and 5/65/35 PMN/PT ceramics is correlated with the oxygen ion vacancies.

## Experimental

Polycrystalline PLMNTx(x=0, 0.02 & 0.05) ceramic samples were prepared by solid solution route using a mixture of PbO (99.9% purity, Aldrich Chemical Co.), MgO (99.9% purity, Aldrich Chemical Co.), TiO2(99.9% purity, Aldrich Chemical Co.), Nb2O5 (99.9% purity, Aldrich Chemical Co.) and La2O3 (99.99% purity, Aldrich Chemical Co.). Specimens were synthesized by changing Mg/Nb/Ti ratio according to the formula Pb1−x Lax[(Mg1+x/3Nb2−x/3)0.65Ti0.35(1−x/4)]O3. The samples were prepared in two steps using columbite precursor method to minimize pyrochlore phase formation **[19]**. The columbite precursor (MgNb2O6) was prepared by mixing predetermined amount of MgO and Nb2O5 in acetone and calcined at 1100 oC for 2 hours. Next the PbO, La2O3 and MgNb2O6 were mixed in stochiometric amounts and calcined at 800oC for 4 hours. The calcined powders were pelletized under a pressure of 100 MPa to obtain disks of thickness 2 mm and diameter 15mm. The pelletized samples were sintered at 1200 oC for 2 hours in a sealed alumina crucible. Each sintered disk was polished with different grades of emery paper to obtain flat surfaces. Phase analysis of the calcined poweders and sintered pellets was performed by X-ray diffraction (XRD) using Rigaku X-ray diffractometer with Cu K ($\lambda$ = 1.54 Å) from 2$\theta$ =20° to 70° at a scanning speed of 0.05o/min with a step size of 0.02°. Densities of the sintered specimens were measured by Archimedes principle. Scanning electron micrographs of the transverse microstructure and grain size were obtained by using a SEM model JEOL-JSM 6360. For electrical measurements high temperature curing silver paste were applied on the opposite faces of the sample and low field amplitude dielectric and impedance spectroscopic measurements were carried out on the samples using Solartron impedance analyzer in the frequency range (1 Hz -1 MHz) and temperature range (30o – 450oC). The temperature was measured with an accuracy of 1 oC. Ferroelectric properties were evaluated by hysteresis loops using Radiant Technologies RT66A Ferroelectric Test System. The hysteresis loops were recorded at a frequency of 50 Hz.

## Results and discussion

### *Structure analysis*

**Fig. 1** (a) shows the x-ray diffraction patterns of PLMNTX(x=0, 0.05, 0.07) ceramics. 65/35

PMN/PT crystallizes in perovskite structure. Here lead (Pb) ions are at the corners of the cube while oxygen(O) are at the face centers and titanium (Ti) is placed at the body center. The crystal structure was identified to be tetragonal (P4mm) and lattice parameters were calculated to be a=b= 4.00154 Ao and c =4.03422Ao in case of pure 65/35 PMN-PT .The lattice parameters for 2/65/35 PMN/PT and 5/65/35 PMN/PT were a=b=4.003 $A^o$ and c =4.016$A^o$ and a=b=4.004$A^o$ and c =4.025 $A^o$ respectively .

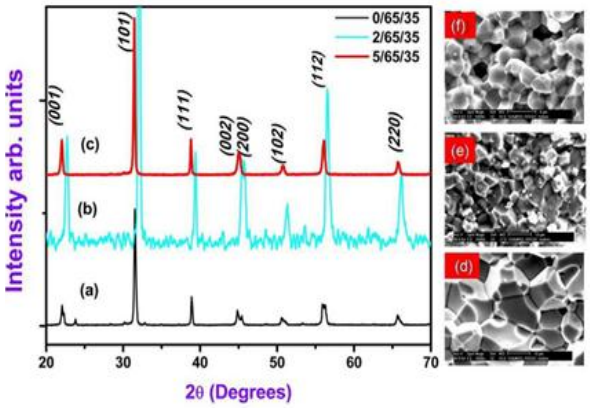


**Fig. 1.** X ray diffraction patterns of (a) 65/35 (b) 2/65/35 (c) 5/65/35 PMN/PT ceramics SEM micrographs of transverse section of (d) 65/35, (e) 2/65/35 and (f) 5/65/35 PMN/PT ceramic samples.

No trace of pyrochlore phases were observed within the uncertainty of XRD. This is in agreement with the JCPDS file no. 01-088-1864. Fig(1(a) -1(c)) indicates the XRD curves of PLMNTX(x=0.0, 0.02,0.05) respectively. A perfect solid solution has formed with no concomitant change in phase or additional phase. The peak at 45o in case of PMN-PT; 65/35 indicated splitting indicating a tetragonal phase of PMN-PT, whereas in case of lanthanum modified PMN-PT no splitting can be observed confirming pseudocubic phase. This also proves the gradual change from the tetragonal to the pseudocubic phase indicating increasing relaxor nature by lanthanum addition .

The transverse microstructure of the PLMNTX(x=0, 0.05, 0.07) pellets are shown in the Fig. 1(d)-1(e). No pyrochlore phase was visible and sharp grain boundaries with highly dense structure were visible. The grain size steadily decreased from 10-12 μ for 65/35 PMN/PT to 4-5 μ for 5/65/35 PMN/PT. The decrease of grain size due to lanthanum doping was due to suppressed grain growth in perovskite structure leading to lower diffusivity **[20]**.

### *Dielectric behavior*

Broad frequency dependent dielectric relaxation peaks are observed in ε/, ε//and tanδ (f) in the frequency range from 100 Hz to 1 MHz indicating typical relaxation behavior for all the compositions. **Fig. 2** shows the temperature dependance of real part of permittivity ε/(f) and dissipation factor tanδ (f) for PMN-PT and PLMNTx (x=0.0, 0.02 & 0.05) samples respectively. Although we did measurements at 20 different frequencies data of only four frequencies are presented for the sake of convenience. The room temperature ε/ and tan δ of the 65/35, 2/65/35 and 5/65/35 PMN/PT samples are 3250, 2575, and 2234 whereas the tan δ values are 0.021, 0.056, 0.043 respectively at 1 kHz. The observed data is in good agreement with the previous literature **[21]**.

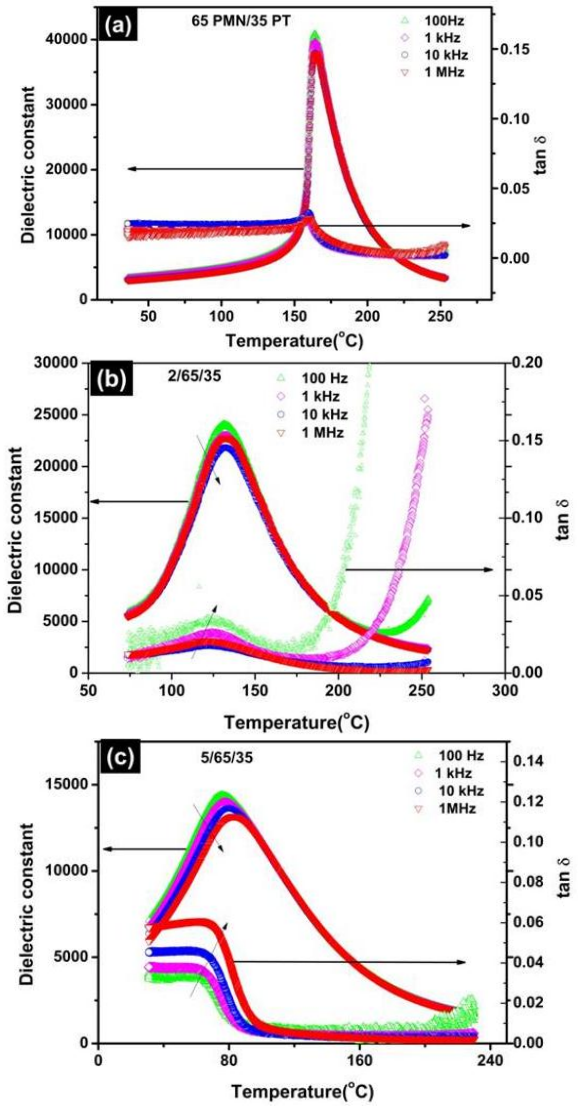


**Fig. 2.** Frequency dependance of the real part of dielectric constant (ε/) and loss tangent tan(delta) with temperature of (a) 65/35, (b) 2/65/35 and (c) 5/65/35 PMN/PT ceramics.

The real part of dielectric permittivity showed clear paraelectric to ferroelectric phase transition in PLMNTx (x=0, 0.02 and 0.05). The dielectric constant for different compositions at curie

Copyright © 2016 VBRI Press 

temperature, Tc for 1 kHz frequency can be summarized as follows ε/(PMN/PT; 0/65/35.)≈ 40,000; ε/ (La/PMN/PT; 2/65/35); ≈23,000; ε/ (La/PMN/PT; 5/65/35) ≈ 14,000. Reduction in dielectric constant is observed with subsequent lanthanum doping. Reduced dielectric constant with increased lanthanum doping is due to the reduced c/a distortion which leads to low polarization and a small grain size as the small grain size leads to multiple grain boundaries leading to blocking of the movement of the polar nanodomains in the grains. Since the dielectric permittivity is related to the free dipoles oscillating in an alternating field hence the blocking motion leads to reduced dielectric constant.

A corresponding decrease in curie temperature, Tc is observed with increasing lanthanum content in PLMNTx (x=0.0, 0.02 & 0.05) ceramics. The corresponding Tc values are (Tc =164 $^{o}$C ; 65/35 PMN/PT), (Tc=131$^{o}$C; 2/65/35 PMN/PT) and (Tc= 77$^{o}$C; 5/65/35 PMN/PT). The decrease in Tc is attributed to the decrease in the tetragonal distortion leading to less thermal energy to overcome lattice distortion.

While 65/35 PMN/PT ceramic sample showed normal ferroelectric behaviour with no dispersion in dielectric constant, difference is observed in the low frequency and high frequency relaxation behaviour of 2/65/35 and 5/65/35 PMN/PT ceramic is indicative of relaxor nature. The low frequency behaviour shows a wide spectrum of relaxation times. Relaxor ferroelectric obey modified curie weiss version of the curie weiss law **[22]**.

$$1/\varepsilon = 1/\varepsilon_m + B(T - T_m)\gamma$$

where, $\varepsilon_m$ the dielectric permittivity at the temperarute Tm and B is is the recoiprocal of the conventional curie weiss constant. The exponent $\gamma$ is equal to unity for a normal ferroelectric. For relaxors it varies between 1 & 2 and its deviation is a measure of the degree of the relaxor nature of the ferroelectric. Dielectric permittivity data fitted using modified curie weiss law has indicated that y value has steadily increased from $\gamma$ = 1.65 for 0/65/35 to $\gamma$ = 1.82 for 2/65/35 and $\gamma$ = 1.99 to 5/65/35 ceramics.

ε/ of samples with frequency at different temperatures (37 $^{o}$C to 250 $^{o}$C) indicates Dispersion occuring in the low and high frequency regime could be attributed to either the space charge polarization, Maxwell Wagner, long range structural order and defect relaxations however dispersion occuring in the present case is due to relaxor nature. No traces of space charge polarization were visible. The value of ε/ is almost constant at all temperatures for measured frequency range. The value of ε/ increases as temperature increases in case of all samples The increase of ε/ with the rise in temperature over the entire frequency range is attributed mainly to the interfacial polarization due to accumulation of charge at grain boundaries and dipolar polarization both of which are strongly temperature dependent. At low frequencies the dielectric constant is high due to the response of electronic, ionic, dipolar and space charge polarization. However at high frequencies only dipolar polarization responds leading to a decrease in dielectric constant.

Such high dielectric constant has emerged due to domain polarization. The orientational polarization in PLMNTx=0-0.05 arises due to the reorientaion of nano dipoles formed due to charge imbalance.

**Fig. 2** also shows the variation of dielectric loss tangent, tanδ with frequency at different temperatures. Broad and prominent relaxation peaks are observed in the temperature range from 30oC to 250 C and frequency range from 100 Hz to 1MHz in PLMNTx (x=0, 0.02, 0.05) ceramics. The dissipation peaks in tan δ are masked by conductivity losses in 2/65/35 PMN/PT ceramics. The relaxation peaks may be due to the oxygen ion jump relaxation, point defects, dipolar relaxation or space charge relaxation [23]. Activation energy and relaxation time calculated from the relaxation peaks of the tanδ curves indicate the values to be 1.25 ev, 1.52 ev and 1.57 eV suggests that the phenomenon is due to the short range hopping of the nano dipoles formed.

The tanδ reduces on lanthanum doping as indicated in **Fig. 2**. On substitution of Lanthanum, there is decrease in concentration of relaxation units ie oxygen vacancies according to the point defect relaxation theory which leads to the decrease in loss tangent **[24]**.

### *Ferroelectric measurements*

**Fig. 3** shows plots of field induced polarization hysteresis (P-E) loops of 0/65/35, 2/65/35 and 5/65/35 samples measured at 50Hz at respectively. Well saturated ferroelectric loops of 0/65/35, 2/65/35 and 5/65/35 PMN/PT have been observed at room temperature due to low leakage current. Such loops are called 'fat' if they enclose a large area, and 'slim' in the opposite case. Normal ferroelectrics exhibit fat loops, and relaxor ferroelectrics exhibit slim loops. Thus, relatively speaking, the slimness is a qualitative indicator of the extent of relaxor character. In case of relaxor ferroelectric the remanent polarization does not go to zero at the permittivity maximum but inflects and tails to zero which shows a typical relaxor characteristic **[4]**. While 65/35 and 2/65/35 PMN/PT exhibited fat loop characteristic of normal ferroelectric, 5/65/35 PMN-PT ceramics exhibited slim

Copyright © 2016 VBRI Press 

ferroelectric loops indicative of relaxor nature. The maximum polarization (Ps) values obtained for 65/35, 2/65/35 and 5/65/35 are 31.6 μC/cm$^2$, 27.1 μC/cm$^2$, and 14.5 μC/cm$^2$ at room temperature respectively. Lanthanum addition in PMN-PT have decreased the coercive field, hysteresis loss, remanent polarization and saturation polarization. The remanent polarization (Pr) and coercive field (Ec) for 0/65/35 at room temperature were 21 μC/cm$^2$, and 5.6 kV/cm which decreased to 3.6 μC/cm$^2$, and 1.9 kV/cm as the temperature increased from 300 $^0$C to 180 $^0$C.

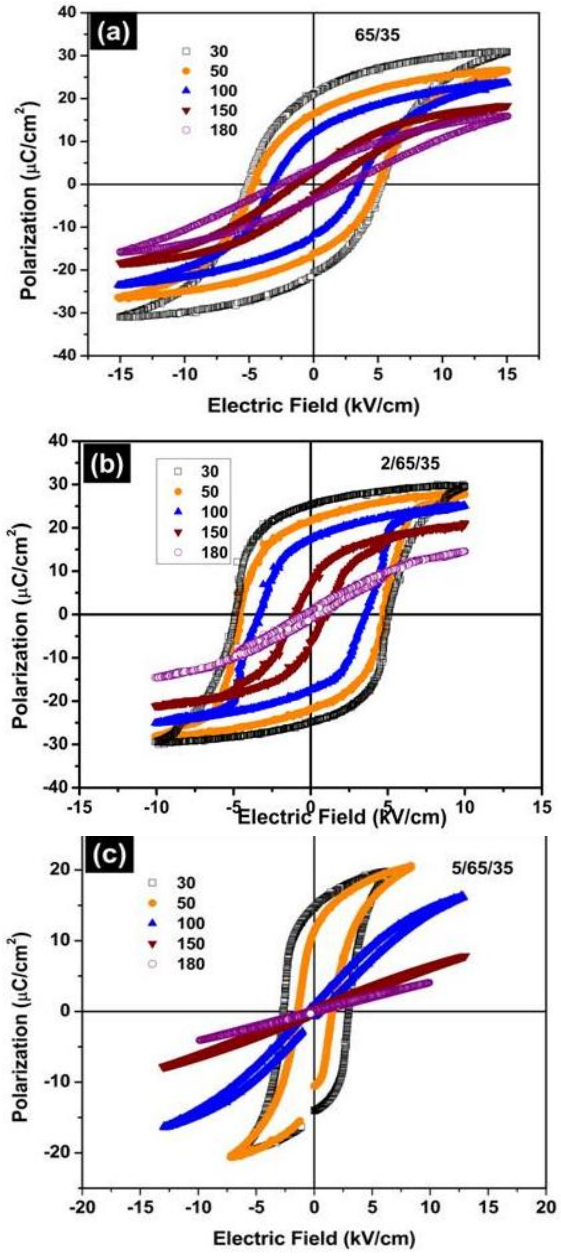


**Fig. 3.** Polarization Hysteresis loops of (a) 65/35, (b) 2/65/35 and (c) 5/65/35 PMN/PT ceramics.

For 2/65/35 ceramics the Pr and Ec varied from 19.3 to 1.4 μC/cm$^2$ and 4.62 kV/cm to 0.5 kV/cm on increasing the temperature from 300 C to 1800C whereas for 5/65/35 ceramics the Pr decreased from 14.5 μC/cm2, to almost 0.5 μC/cm$^2$, and Ec decreased 2.9 kv/cm to 0.2 kV/cm. This field induced ferroelectrc polarization and almost negligible remanent polarization can be explained by considering nanopolar regions. The system tries to cope with the local charge imbalance by forming nanoclusters of ordered regions, separated by disordered regions. These nanoclusters are so small that thermal fluctuations are able to flip them around, and when this flipping occurs, even their sizes fluctuate. Thus there exist ferroelectric nanodomains (polar nanoregions), with dynamically changing boundaries. At temperatures above the Burns temperature (Td), thermal fluctuations are so strong that even the nanoclusters do not get formed substantially. As the temperature is lowered below Td, the average size of the nanoregions grows, as does the value of the electric polarization, Ps , associated with each nanoregion. However, since the nanosized clusters are flipped around by the thermal fluctuations, the quantity Pr, averaged over all the directions, is zero.

***Modulus spectra analysis***

Impedance spectroscopy is the measurement and analysis of some or all of the impedance related functions Z* (Impedance), Y* (Admittance), M* (Modulus) and ε* (Permittivity). The electrical homogeneity in the samples can be modeled by the various spectroscopic plots i. e. Z//(imaginary part of Z*) vs frequency and M// (imaginary part of M*) vs frequency. Generally Z * and Y* are used to extract R values and ε* and M* are used to extract C values. The Z* plots terminate at the origin at the high frequencies whereas the M* plots commence at the origin of the low frequencies. Any equivalent circuit consisting of some combination of R and C element connected in series or parallel models the impedance spectroscopy data or it represents physically the various charge migration and polarization phenomenon occurring in the ceramic. Different RC elements represent the electrical responses of grain, grain boundary and various contact impedances. Each parallel RC circuit should give rise to a semicircle in the Z/ vs Z// and M/ vs M// plots and to a Debye peak in the spectroscopic plots of the imaginary components of Z// and M// vs log f where as a Debye type response is treated in terms of a simple RC circuit. A constant phase element (CPE) element is normally represented in form of a depressed semicircle. Normally the grain boundary act as the barrier for the cross transport of the charge carriers and the barrier character of the grain boundary is especially pronounced in the low temperature regime. There may be both frequency dependent relaxations

Copyright © 2016 VBRI Press 

associated with the grain boundaries or there would be dielectric losses associated with the reorientation of dipoles present in the sample. Impedance spectra are dominated by the most resistive components in the sample whereas the modulus spectra are dominated by those components having the largest volume fraction. Often the peaks are seen in modulus spectra which are hidden in the corresponding impedance spectra.

**Fig. 4** represents the frequency dependence of the imaginary part of Modulus (M") (normalized values M"/M"max) in the range from 1Hz to 1 MHZ at different temperatures for PLMNTx(x=0, 0.02, 0.05) ceramics is shown in the figure respectively.

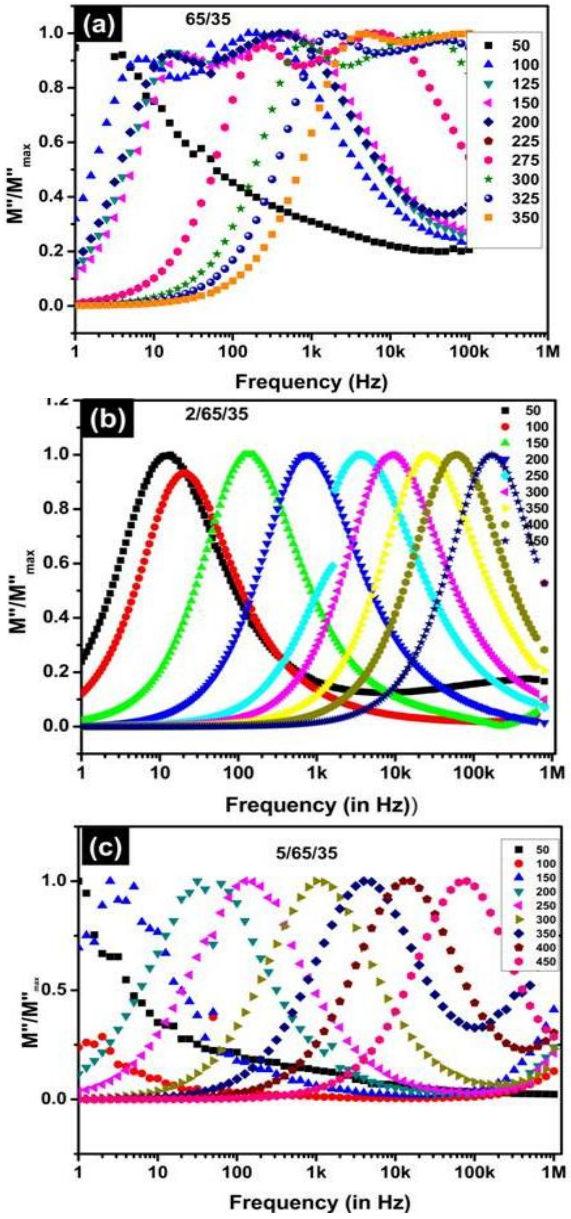


**Fig. 4.** Variation of normalized modulus (M///M//max) with frequency at various temperatures for (a) 65/35, (b) 2/65/35, and (c) 5/65/35 PMN/PT ceramics.

Modulus plots are broader than 1.414 decades indicating deviation from ideal Debye behavior .The maxima of the M// are shifted towards higher relaxation frequencies with the rise in temperature indicating decrease in relaxation time. The mean relaxation time for the complex modulus plots were found to be in the range of 10-5 to 10-6 sec.The relaxation time dependence on the temperature is expressed as

$$\tau = \tau_0 \exp\left(E_R / kT\right)$$

The values of the activation energies calculated from relaxation curves for 65/35, 2/65/35, 5/65/35 PMN/PT ceramics lies between 1.27 eV, 1.25 ev and 1.57 ev which is the activation energy corresponding to the motion of the oxygen vacancies. The appearance of a single arc in the spectrum in the temperatures range of 2/65/35 and 5/65/35 from 50 $^{o}$C to 450 $^{o}$C confirm that only the bulk relaxation is highlighted and grain boundary effects tend to be eliminated whereas in case of 65/35 PMN/PT ceramics both grain and grain boundary contributions were visible. The depressed semicircle in the complex modulus spectra refers to the deviation from the ideal Debye behavior which indicates multiple relaxations occurring within the bulk. Since there is a systematic shift in the peak frequency with temperature it further emphasizes the possibility of presence of multiple equilibrium states with a distribution of relaxation times. The shape of the modulus spectroscopic plots obtain at different temperatures remain the same hence the distribution of the relaxation time is independent of the temperature.

***Impedance measurements***

**Fig. 5** shows the variation in the imaginary part of impedance (Z") as a function of frequency at various temperatures. A decrease in impedance with temperature and frequency in, PLMNTx (x = 0, 0.02, 0.05) is suggestive of decreasing impedance with increasing temperature in the samples. This behaviour can be attributed to the dc conductivity predominant at higher temperature. Also broad relaxation peaks are observed in Z" spectroscopic plots in 65/35,2/65/35 and 5/65/35 PMN/PT ceramics which shift towards higher frequency with increase in temperature. These relaxation peaks are indicative of some relaxation phenomenon either due to charge carriers, defects or dipole relaxation. The activation energy for the relaxation peaks are observed in the range of 0.89 ev which are similar to modulus relaxation peaks indicating that similar phenomenon is responsible for relaxtion process.

Copyright © 2016 VBRI Press 

***Electrical conductivity***

**Fig. 6**(a), 6(b) & 6(c)) demonstrates the variation of real part ac conductivity with frequency at different temperatures for PLMNTX(x=0, 0.02 and 0.05) ceramics. At low temperature ac conductivity is found to be both temperature and frequency dependent, however at higher temperatures (>300 $^{o}$C) it is almost constant.

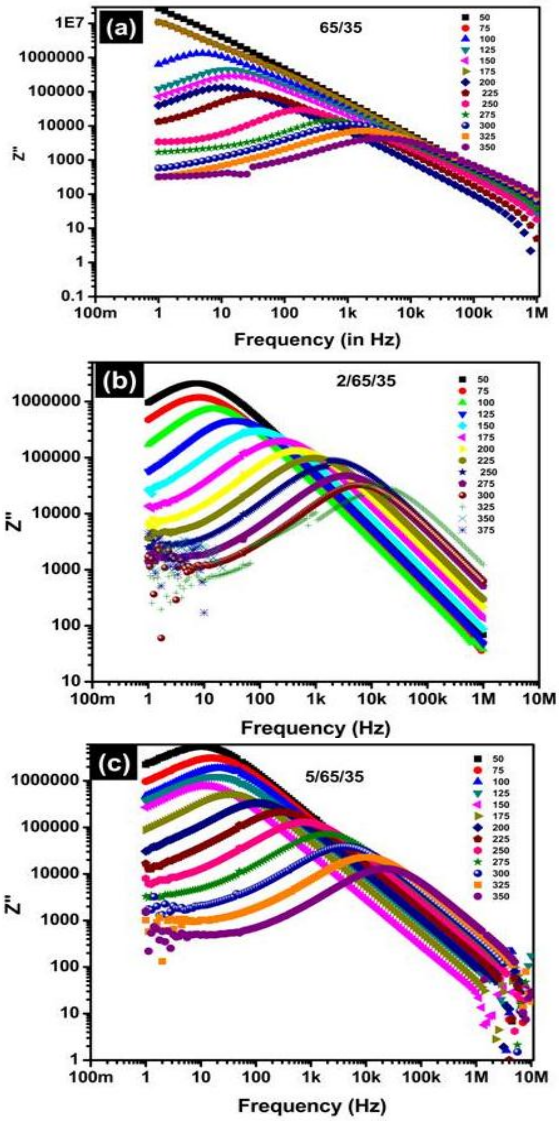


**Fig. 5.** Spectroscopic impedance plots of (a) 65/35 (b) 2/65/35 and (c) 5/65/35 PMN/PT ceramics measured at different temperatures.

For a particular temperature the ac conductivity increases with frequency however below a certain frequency (<1 kHz) the conduction is basically dc conduction. The origin of dc conductivity and ac conductivity mainly depends on motion of different types of charge carriers and details about the charge carriers can be explained from activation energy of the charge carriers.

The angular dependence of the real ac electrical conduction is well described by the equation

$$\sigma'(\omega) = \sigma\ (dc) + A\omega n$$

where, $\sigma\ (o)$ is the independent frequency conductivity or dc conductivity which is related to the drift of the charge carriers and follows Arrhenius equation.

$$\sigma(T) = \sigma_0 \exp\left(-E_a/kT\right)$$

where, $E_a$ is the activation energy for electrical conduction and $\sigma_0$ is the pre-exponential factor. The frequency dependent ac component is given by

$$\sigma_2(T) = A(T)\omega^n(T)$$

The exponent η indicates how σ varies with frequency. The exponent η is such that (0<η<1). This behavior is characteristics of the charge transport in disordered materials and is interpreted by Johnscher as universal dynamic response.

The variation of η with temperature suggests the conduction mechanism of the process **[25, 26]**. Different models have been developed to explain the ac conductivity of oxide ceramics. Some of the most prominent models are Quantum Mechanical Tunneling (QMT), Correlated Barrier Hopping (CBH) and Overlapping Large Polaron tunneling (OLPT) model. According QMT model, η should be independent of temperature **[27]**, whereas CBH predicts a decrease in η with increasing temperature **[28]**. If η increases with the temperature, small polaron conduction is predominant **[29]**. A minimum value of η followed by an increase suggests that the conduction mechanism is due to an overlapping large polaron tunneling mechanism **[30]**.

The value of n obtained from the graphs decreases from 0.532 to 0.21 in the temperature range from 100 $^{o}$C- 300 $^{o}$C for 65 PMN/35PT, from 0.647 to 0.201 in the temperature range from 80 $^{o}$C to 300 $^{o}$C for 2/65/35. While in case of 5/65/35 it has decreased from 0.446 to 0.321 in the temperature range from 70 $^{o}$C to 250 $^{o}$C.

The obtained values of η from the experimental data from $PLMNT_X$(x=0, 0.02 and 0.05) samples are found in agreement with the (CBH) model.

**Fig. 6(d), 6(e)** and **6(f)** shows the Arrhenius plots of ac conduction at different frequencies. The dependence of ac conductivity on temperature is explained by the Arrhenius equation.

$$\sigma(T) = \sigma_0 \exp\left(-E_a/kT\right)$$

At high temperatures (region –I, **Fig. 6**) $\sigma_{ac}$ shows a faster rise with increasing temperature At low temperatures, $\sigma_{ac}$ is almost constant at any fixed frequency (region-II of **Fig. 6**). In the region II, there is strong frequency dispersion for all samples and $\sigma_{ac}$ increases with increase in frequency. In region I the conductivity is mainly controlled by dc conduction mechanism in the sample. In region II strong frequency dispersion may be attributed to the

Copyright © 2016 VBRI Press 

hopping movement of oxygen charge carriers among different perovskite sites having variable barrier heights and separation. From **Fig. 6** (for region I, considering Arrhenius behavior) the activation energies for intrinsic conduction at different frequencies have been calculated for PLMNTx presented in **Table 1**.

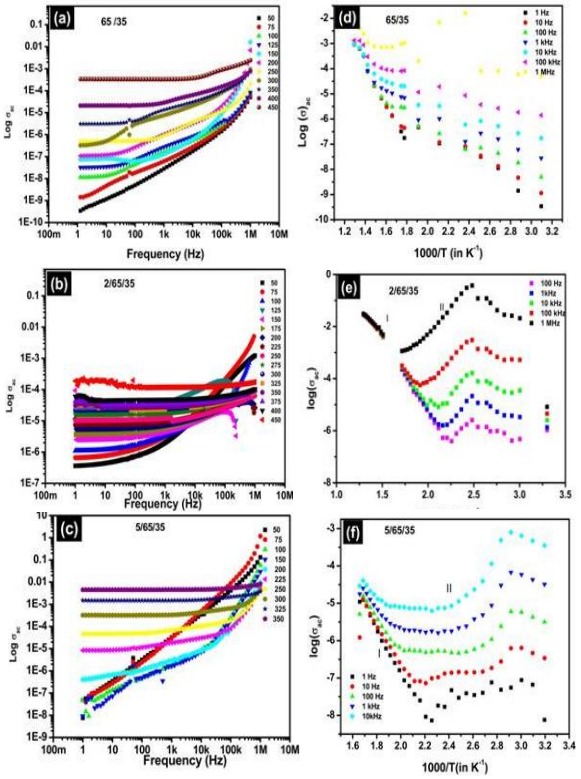


**Fig. 6.** Frequency dependent ac conductivity data for (a) 65/35 (b) 2/65/35 and (c) 5/65/35 PMN/PT ceramics at different temperatures. Plots of ac conductivity vs 1000/T(oK) for (a) 65/35 (b) 2/65/35 and (c) 5/65/35 PMN/PT ceramics at different frequencies.

The activation energy do not significantly change with frequency from 100 Hz to 1MHz in case of 65/35, 2/65/35 and 5/65/35 PMN/PT ceramics. The typical values of the ac activation energies at high temperature indicate ionic conduction due to motion of the doubly ionized oxygen vacancies. The activation energies in region I for 65/35, 2/65/35 and 5/65/35 PMN/PT ceramics at 100 Hz are 1.42, 0.89 and 1.10 ev respectively which indicates ionic conductivity due to doubly ionized oxygen vacancies. The temperature dependence of the dc conductivity of the $PLMNT_X$ (x=0, 0.05 and 0.07) ceramics is shown in the **Fig. 7**. Two different conduction mechanism has been identified for dc conductivity. At high temperature the intrinsic conduction due to oxygen vacancy motion dominates which is indicated by the activation energy in region I whereas the activation energies for dc conductivity are 1.46, 1.01 and 1.21ev respectively (**Table 1**). The ac activation energies are comparable to the dc activation energies. A comparison of the ac conductivities of the different ceramic samples indicated that ac conductivity increased on adding 2 mol% of La and it decreased on further adding 5 mol% of La as indicated in Fig 6(b). This behaviour of ac conduction can be explained by taking into account the conduction behaviour of perovskites. PMN-PT basically belongs to ionic conductivity though it may be tantamount to slight electronic conductivity due to multivalent oxidation state of $Ti^{3+}$ $Ti^{4+}$. Ionic conductivity in PMN-PT ceramics is due to (a) cation vacancies ($Pb^{+2}$) due to vaporization of PbO; (b) oxygen vacancies created due to vaporization of PbO ;

$$Oo = 1/2\ O_2 + V_0 + e^-$$

On doping La, it gets is incorporated in the $Pb^{2+}$ site in the pervoskite phase. Doping of trivalent $La^{3+}$ for divalent $Pb^{2+}$ causes charge imbalance which is compensated by the formation of A site vacancies.

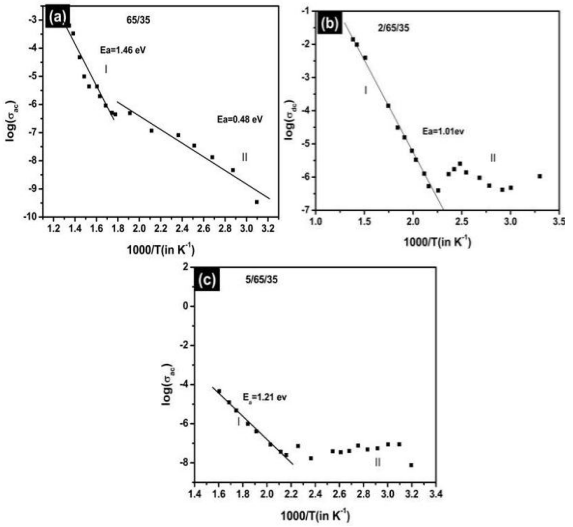


**Fig. 7.** Arrhenius plots of the dc conductivity for (a) PMN/PT, (b) 2/65/35 and (c) 5/65/35 PMN/PT ceramic.

**Table 1.** Activation energies Eac, Edc (eV) and ac conductivity for PLMNTx(x=0.0, 0.02, 0.05) ceramics

| Sample | Region (II) Eac (eV) 1Hz | 100 Hz | 1KHz | 10 KHz | 1 MHz | σac (Ω-1cm$^{-1}$) at 80 K at 1kHz | σac (Ω-1cm-1) at 300 K at 1kHz | σdc (Ω-1cm-1) at 80 K | Edc (eV) Region (I) | Region (II) |
|---|---|---|---|---|---|---|---|---|---|---|
| 65PMN/35/PT | 1.48 | 1.42 | 1.27 | 1.27 | 1.28 | 2.7893E-8 | 7.57686 E-6 | 3.4320E -10 | 1.46 | 0.48 |
| 2/65/35PMN/PT | 1.10 | 0.84 | 0.71 | 0.71 | 0.61 | 1.9987E-5 | 2.24245 E-5 | 3.6377E -7 | 1.01 | -- |
| 5/65/35PMN/PT | 1.25 | 1.10 | 0.96 | 0.96 | 0.84 | 4.3040E-6 | 1.2656E -6 | 6.6349E -9 | 1.21 | -- |

Copyright © 2016 VBRI Press 

$$La_2O_3 = 2La^{*}_{Pb} + 3O^{*}_{o} + V''_{pb}$$

where, represents $La^{*}_{Pb}$ a lanthanum ion on the lead site with one effective positive charge, $O^{*}_{o}$ represents an oxygen ion in oxygen without any effective charge and $V''_{pb}$ represents lead vacancies with two effective negative charges. Doping of 2 mol% of La leads to generation of both oxygen and cation vacancies resulting in an increase in ionic conductivity however on further doping of 5 mol% of La the oxygen ion generated by $La_2O_3$ would occupy oxygen vacancies resulting in the reduction of conductivity.

## Conclusion

Single phase $PLMNT_X$ (x=0, 0.02 &0.05) ceramics were fabricated by conventional solid solution route using columbite precursor method. The crystal structure of 65/35 PMN/PT ceramic changes from tetragonal P4mm to pseudocubic Pm3m on being doped by $La^{3+}$. The dielectric permittivity and curie temperature, Tc of 65/35 PMN/PT is decreased when it is doped with 2 mol% and 5 mol% of lanthanum. The values of the activation energies and the relaxation nature of the modulus spectroscopic curve suggested the relaxation process to be governed by the thermal motion and hopping of oxygen ion vacancies. The variation of the frequency exponent η with temperature in the frequency dependent ac conductivity component indicates that ac conduction in ceramics is due to correlated barrier hopping mechanism of charged species. The activation energies ($E_a$) of PLMNTx(x= 0, 0.02 and 0.05) ceramics for ac conductivity at 100 Hz are 1.42, 0.89 and 1.10 ev respectively. This indicates in these ceramics oxygen ion vacancies contribute to long range and short range conduction.

### Acknowledgements

The author is greatful to Shri P.S. Parihar, Director AMD for giving permission to publish this paper.

### References

1. Park S. E.; Shrout T. R.; *J. Appl. Phys*., **1997**, *82*, 1804. **DOI:** http://dx.doi.org/10.1063/1.365983
2. Shrout T. R.; Fielding Jr. J; *Proc. IEEE*, **1964**, *35*, 711. **DOI:** http://dx.doi.org/10.1109/ULTSYM.1990.171456
3. Cross, L.; Jang, S.; Newnham, R.; Nomura, S., Uchino, K., **1980**, *23*, 187. **DOI:** http://dx.doi.org/10.1080/00150198008018801
4. Pandit, P.; Wadhawan, V. K.; Gupta, S. M.; *Smart Mater. Struc.*, **2006**, *15*, 653. **DOI:** http://dx.doi.org/10.1080/00150198008018801
5. Pandit, P; Wadhawan, V. K.; Gupta, S. M.; *Smart Mater. Struc.*, **2007**, *16*, 1246. **DOI:** http://dx.doi.org/10.1088/0964-1726/16/4/036
6. Noheda, B.; Cox, D. E.; Shirane, G.; Z.-G. Ye; Gao, J; *Phys. Rev. B*., **2002**, *66*, 054104. **DOI:** http://dx.doi.org/10.1103/PhysRevB.66.054104
7. Ye, Z. G.; Noheda B. ; Dong, M.; Cox, D.; Shirane, G.; *Phys. Rev. B*., **2001**, *64*,184114. **DOI:** http://dx.doi.org/10.1103/PhysRevB.64.184114
8. Kiat, J. M.;, Y. Uesu, B. Dkhil, M. Matsuda, C. Malibert, Calvarin G. ; *Phys. Rev. B*., **2002**, *65*, 064106. **DOI:** http://dx.doi.org/10.1103/PhysRevB.65.064106
9. Shaw J.C. ; Liu K. S.; *I. N. Lin Scripta Metall. et Material*, **1993**, *29*,981. **DOI:** http://dx.doi.org/10.1016/0956-716X(93)90394-8
10. Blinc, R.. ; Dolinˇsek, J.; Gregoroviˇc, A.; Zalar, B.; Filipiˇc, C.; Kutnjak, Z.; Levstik, A.; Pirc, R., Phy.Rev.Lett. 1999, 83,424 **DOI:** http://dx.doi.org/10.1103/PhysRevLett.83.424
11. Pirc, R.; Blinc, R; *Phys. Rev. B*., **1999**, 60, 13470. **DOI:** http://dx.doi.org/10.1103/PhysRevB.60.13470
12. Ghosh V J; Nielsen B; Friessnegg T.; *Phys. Rev. B*., **2000**, *61*, 207. **DOI:** http://dx.doi.org/10.1103/PhysRevB.61.207
13. Badillo, F.A.N.L.; Eiras, J. A.; Milton, F. P; Garcia, D; *Opt. Photonics J*., **2012**, *2*, 157. **DOI:** http://dx.doi.org/10.4236/opj.2012.23023
14. James A. R.; Srinivas K; *Mater. Res. Bull*, **1999**, *8*, 1301. **DOI:** http://dx.doi.org/10.1016/S0025-5408(99)00127-0
15. James, A. R.; Priya, S. ; Uchino K., ; Srinivas, K; *J. Appl. Phys.*, **2001**, *90*, 3504. **DOI:** http://dx.doi.org/10.1063/1.1401802
16. Gupta S. M.; Prasad N. V. ; Wadhawan V. K.; *Ferroelectrics*, **2005**, *326*, 43. **DOI:** http://dx.doi.org/10.1080/00150190500318222
17. Macdonald, J. R. (Eds); Impedance spectroscopy Emphasizing Solid Materials and systems, *John Wiley & sons*, **1987**.
18. Johnscher A. K. (Eds); Dielectric Materials in Solids; Chelsea :London **1983.**
19. Swartz, S. L.; Shrout , T. R.; *Mat. Res. Bull.*, **1982**, *17*, 1245. **DOI:** 10.1016/0025-5408(82)90159-3
20. Chou .X; Zhai. J; Jiang, H. ; Yao, X. J.; *Appl. Phys*., 2007, 102, 084106. **DOI:** 10.1063/1.2799081
21. Gupta, S. M.; Pandit, Pragya; Wadhwan, V.K; *Mater. Sci. & Engg. B.*, **2005**, *120*, 125. **DOI:** http://dx.doi.org/10.1016/j.mseb.2005.02.013
22. Uchino K.; Nimura S., *Ferroelectrics*, **1982**, *216*, 11.
23. Singh, G.; Tiwari, V. S.; Gupta, P. K; *J. Appl. Phys*., **2007**, *107*, 064103. **DOI:** http://dx.doi.org/10.1063/1.3309745
24. S. Rachna. ; Bhattacharyya. S. ; Gupta, S. M; *Mater. Sci. & Engg. B.*, 2010, 175, 207. **DOI:** http://dx.doi.org/10.1016/j.mseb.2010.07.029
25. Fayek M. K., Mostafa M. F. Sayedahmed F, Ataallah SS and Kaiser M; *J. Magn. Magn. Mater*., **2000**, *210*, 189. **DOI:** http://dx.doi.org/10.1103/PhysRevB.67.144519
26. Gopalan E. V.; Malini, K.A. ; Saravanan S.; , Sakthi Kumar D.; Yoshida. Y.; Anantharaman M. R.; *J. Phys. D: Appl. Phys.*, **2008**, *41*. **DOI:** http://dx.doi.org/10.1088/0022-3727/41/18/185005
27. Austin, I.G. ; Mott, M.F.; *Adv. Phys*., **1969**, *18*, 41. **DOI:** http://dx.doi.org/10.1080/00018736900101267
28. Elliot S. R.,; *Philos Magn*., **1977**, *36*, 1291.
29. **DOI:** http://dx.doi.org/10.1080/14786437708238517
30. Meaz, T. M. ; Attia, A. M. S. M ; Ata. A. E.; *J.Magn. Mater*., **2003**, *257*, 296. **DOI:** http://dx.doi.org/10.1016/S0304-8853(02)01212-X
31. Ghosh, A.; *Phys. Rev. B*., 1990, 42, 1385. **DOI:** http://dx.doi.org/10.1103/PhysRevB.42.1388

Copyright © 2016 VBRI Press 